INTERNATIONAL JOURNAL OF HYDROGEN ENERGY 38 (2013) 16387–16393

Available online at www.sciencedirect.com

SciVerse ScienceDirect

journal homepage: www.elsevier.com/locate/he

Short Communication

Application of a composite electrolyte in a solid-acid fuel cell system: A micro-arc oxidation alumina support filled with CsH_2PO_4

Xinghua Guo [a], *Keqin Du* [a,*], *Yuxi Huang* [b], *Hao Ge* [c], *Quanzhong Guo* [a], *Yong Wang* [a], *Fuhui Wang* [a]

[a] *State Key Laboratory for Corrosion and Protection, Institute of Metal Research, Chinese Academy of Science, Shenyang, China*

[b] *Shenyang Branch of China Coal Research Institute, China*

[c] *Liaoning Key Laboratory for Green Synthesis and Preparative Chemistry of Advanced Materials, College of Chemistry, Liaoning University, Shenyang, China*

ARTICLE INFO

Article history:
Received 3 July 2013
Received in revised form
10 September 2013
Accepted 20 September 2013
Available online 19 October 2013

Keywords:
Solid-acid fuel cell
High stability
Micro-arc oxidation alumina support

ABSTRACT

A micro-arc oxidation alumina (MOA) support filled with a CsH_2PO_4 proton conductor was investigated as an inorganic composite electrolyte for a H_2/O_2 solid-acid fuel cell (SAFC). The MOA support was polycrystalline and contained α- and γ-Al_2O_3 phases; while, the proton conductor CsH_2PO_4 formed an interlaced network within the MOA support. The single-module SAFC using the fabricated MOA/CsH_2PO_4 membrane delivered a peak power of ~38.5 m W cm^{-2} and a proton conductivity of ~2.1 m S cm^{-1} at a low temperature (25 °C). Compared to a SAFC using an anodic alumina membrane composite electrolyte (AAM/CsH_2PO_4 SAFC), which displayed rapid degradation, the SAFC using the MOA/CsH_2PO_4 composite electrolyte showed improved stability with cycling. This was attributed to the crystalline α-Al_2O_3 phase that was part of the MOA support that had increased the chemical resistance.

1. Introduction

In recent years, new fuel cells based on solid-acid electrolytes, such as the compounds $CsHSO_4$ and CsH_2PO_4, have resulted in higher power density and lower-cost membranes [1–6]. However, pure solid acids are not suitable for large-scale applications due to problems with their water-solubility and mechanical properties. Therefore, a novel composite electrolyte based on an anodic alumina membrane (AAM) and a solid acid was developed and used as a solid-acid fuel cell (SAFC). This type of SAFC has demonstrated considerable viability at low temperatures [7–9]; this is where the AAM acts as a support, and the solid acid ($CsHSO_4$ or CsH_2PO_4) proton conductor is used to fill the AAM. Unfortunately, due to the amorphous AAM support being attacked by the CsH_2PO_4 as a result of local acidification, the performance of the AAM/CsH_2PO_4 SAFC has shown rapid degradation [9]. Subsequently, a neutral salt, i.e., $Cs_{0.86}(NH_4)_{1.14}SO_4Te(OH)_6$, compatible with AAM was prepared, which was stable at room temperature [10].

* *Corresponding author*. Tel.: +86 24 23895348; fax: +86 24 23915894.
E-mail addresses: kqdu@imr.ac.cn, xhguo@imr.ac.cn (K. Du).
0360-3199/$ – see front matter
http://dx.doi.org/10.1016/j.ijhydene.2013.09.127

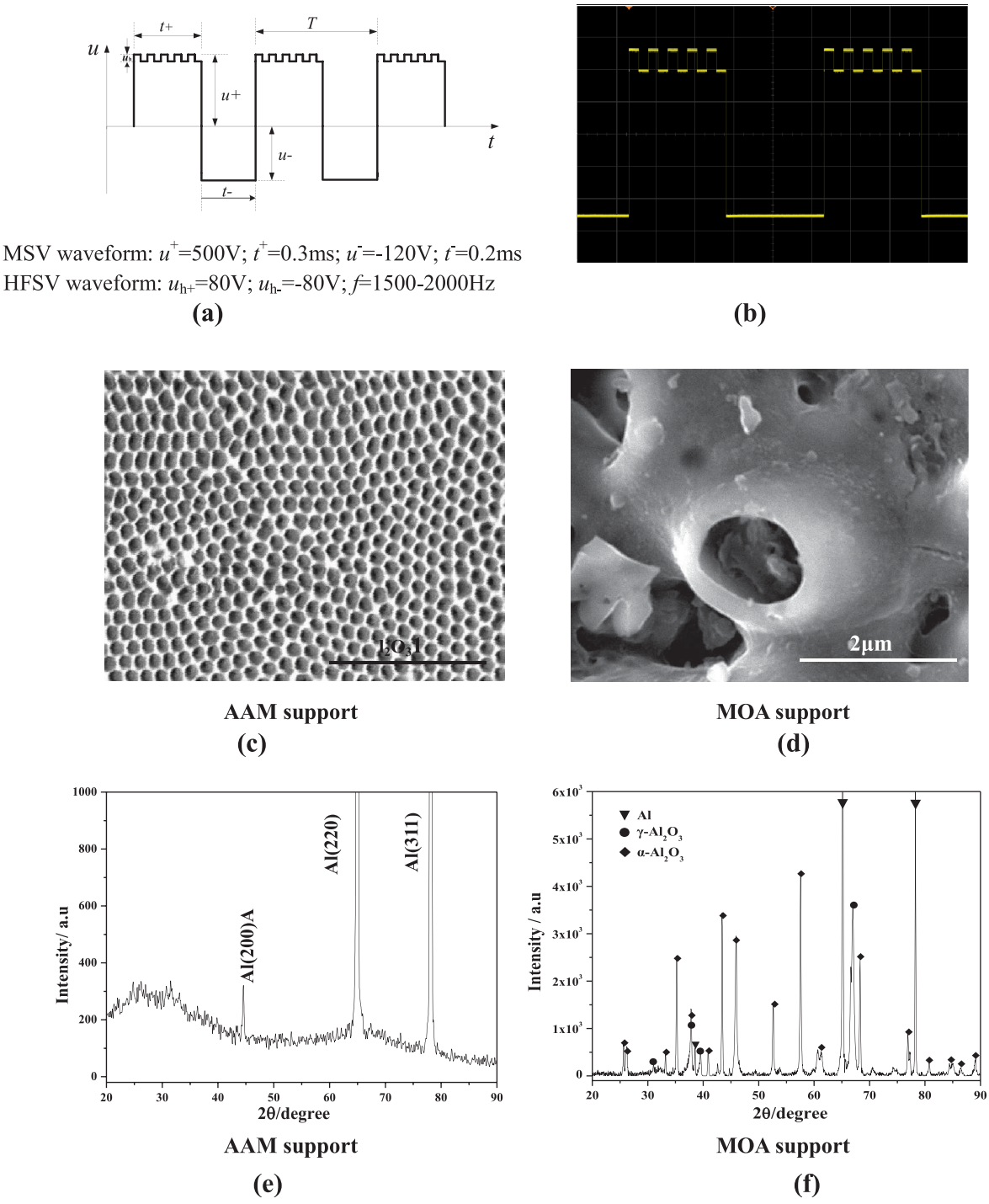

Fig. 1 – (a,b) Oscillograms of the TSFC mode, (c,d) morphologies and (e,f) phases of the AAM and MOA supports, respectively.

In this paper, an acid-resistant support based on a thin micro-arc oxidation alumina (MOA) film fabricated in transient self-feedback control (TSFC) mode was investigated for use as the frame of the composite support/CsH_2PO_4 membrane. Three findings from our previous work have developed our interest in MOA films [11–14]. Firstly, ceramic MOA films have better mechanical strength when they are under a strong electric field. Secondly, porous MOA films can be electrochemically grown to have a wide range of thicknesses (from a few microns to hundreds of microns) and porosities (from about 10% to 30%), with pore diameters ranging from tens of nanometers to several micrometers. These properties can be achieved through using a complex voltage waveform consisting of a matrix square voltage (MSV) waveform and a high-frequency square voltage (HFSV) waveform. Thirdly, when the HFSV waveform frequency was dynamically altered an acid resistant α-Al_2O_3 phase was obtained that had a more stable microstructure. Therefore, in this study, we

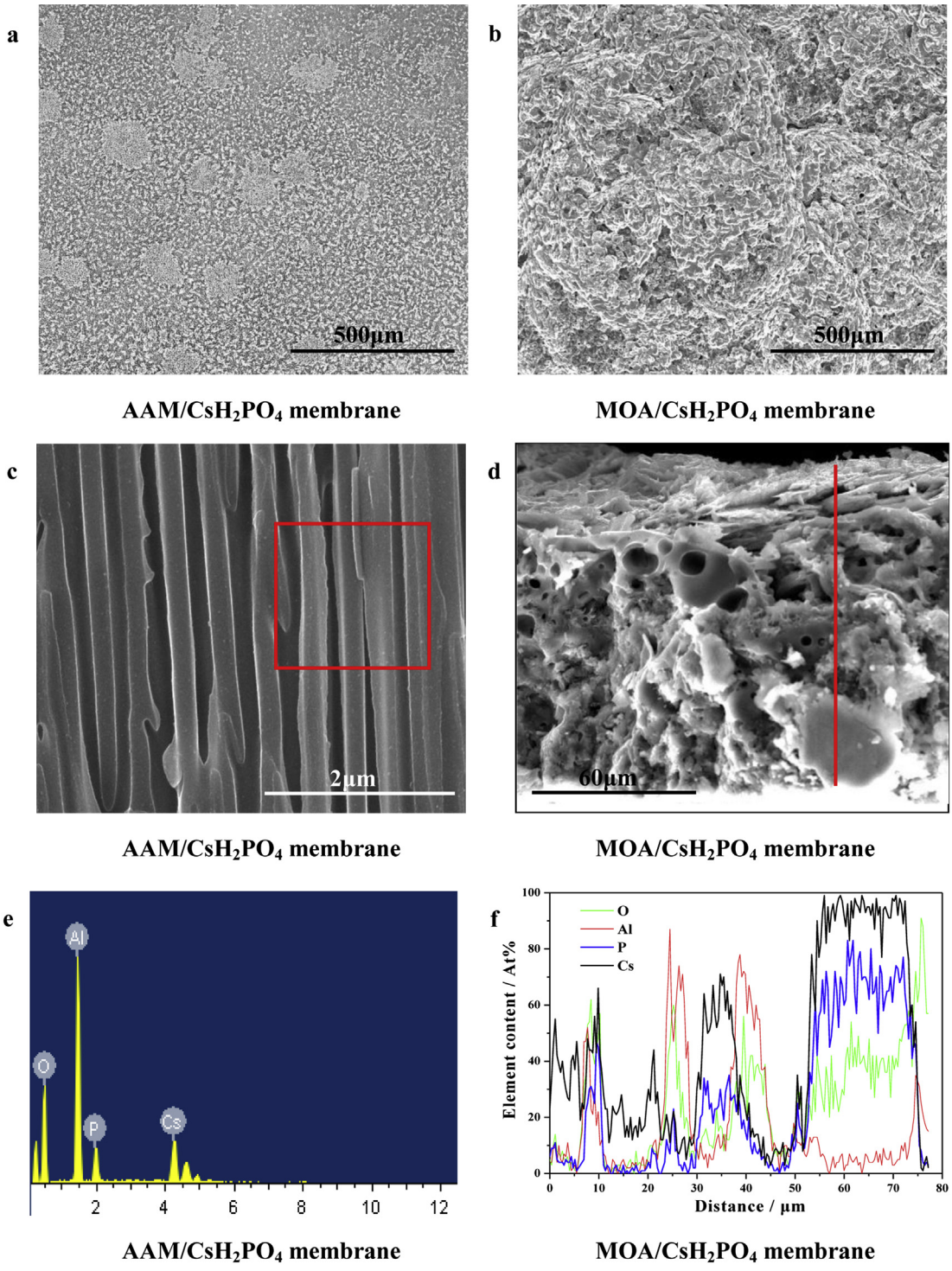

Fig. 2 – (a,b) Surface morphologies, (c,d) cross-sectional morphologies, and (e,f) elemental analyses of AAM/CsH_2PO_4 and MOA/CsH_2PO_4 membranes, respectively.

investigated whether this novel MOA support material would be able to improve the functions of a SAFC. Here we report some properties of the composite MOA/CsH_2PO_4 membrane in a H_2/O_2 SAFC. In addition, an AAM/CsH_2PO_4 membrane was fabricated to act as a baseline against which the MOA/CsH_2PO_4 membrane's electrochemical properties could be compared.

2. Experimental

2.1. *Preparation of supports and composite membranes*

Aluminum sheets (thickness: 0.5 mm; purity: >99.999%) were obtained from Joinworld Co., Ltd. (Xinjiang, China). The AAM

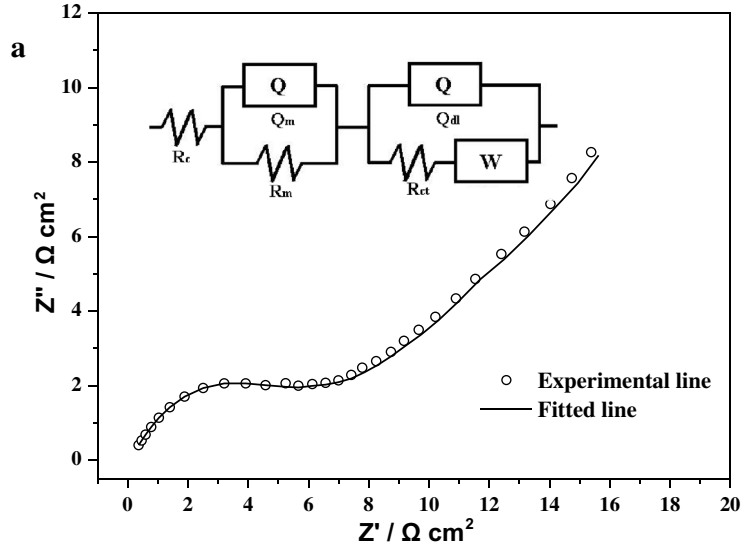
a
Q
Qm
Q
Qdl
W
Rr
Rm
Rct
Experimental line
Fitted line
Z'' / Ω cm2
Z' / Ω cm2

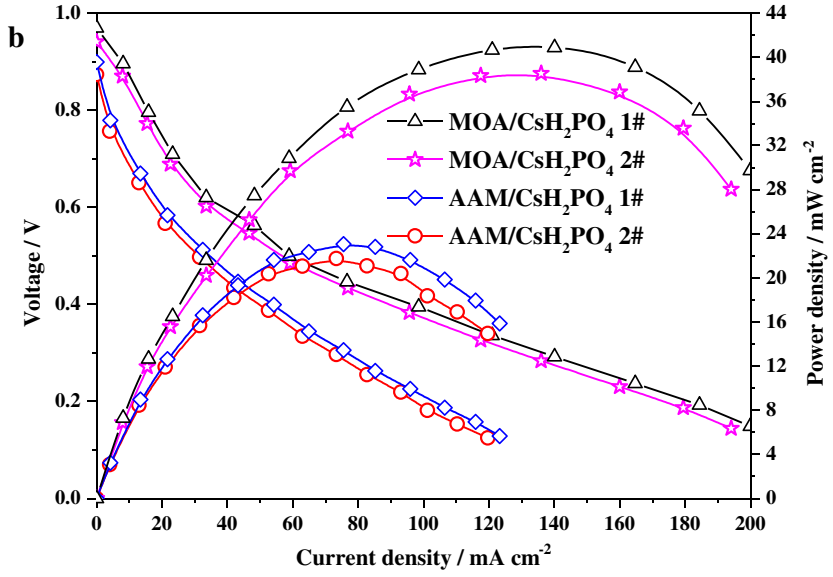
b
MOA/CsH2PO4 1#
MOA/CsH2PO4 2#
AAM/CsH2PO4 1#
AAM/CsH2PO4 2#
Voltage / V
Power density / mW cm-2
Current density / mA cm-2

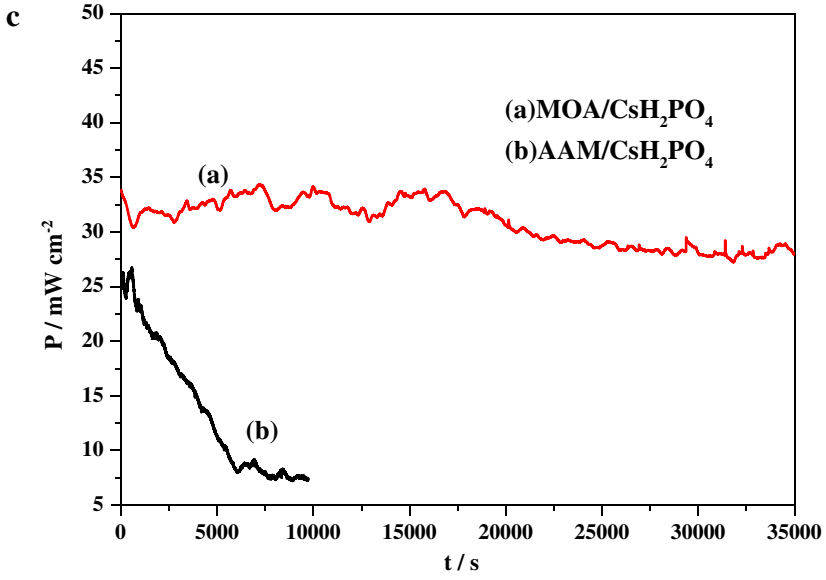
c
(a)MOA/CsH2PO4
(b)AAM/CsH2PO4
(a)
(b)
P / mW cm-2
t / s

support was prepared using a two-step anodization technique following a previously published method [15]. The first and second anodization steps were performed in a 1:1.5 sulfuric/oxalic acid mixture at 20 V and 5 °C for 1.5 h each. After the first anodization step, the formed alumina was etched off in an aqueous solution containing 1.8% CrO_3 (wt%) and 6% H_3PO_4 (wt%) at 60 °C for 2 h. After the second anodization, the remaining aluminum substrate was removed by soaking in a $CuCl_2$-based solution (100 mL of HCl (38%) + 100 mL of H_2O + 3.4 g of $CuCl_2 \cdot H_2O$) at room temperature for ~10 min. The perforated AAM template was prepared by removing the bottom part (barrier layer) of the template in 5% (wt%) H_3PO_4 at 35 °C.

The MOA support was created using a pulse power supply (Duercoat IV), which was able to deliver the monopolar pulse carrier wave described in Refs. [11,12]. The HFSV and MSV waveforms were loaded so that a complex square voltage waveform could be exported (Fig. 1(a) and (b)). The anode was an Al sheet and the cathode was a stainless steel plate. The MOA film processing time was 40 min, and the temperature of the electrolyte was maintained below 35 °C during the entire process using a DuraChill cooling system (PolyScience; Niles, IL, USA). The electrolytes, NaOH (3–5 g L^{-1}), Na_2SiO_3 (2–5 g L^{-1}), and the organic addition agent (1 g L^{-1}) were dissolved in deionized water at room temperature (25 °C). The perforated MOA support was prepared by removing the bottom part (barrier layer) of the membrane in 5% (wt%) H_3PO_4 at 35 °C.

The pores of the as-received membranes or initially treated membranes were filled with CsH_2PO_4. The CsH_2PO_4 solid acid was synthesized from an aqueous solution of Cs_2CO_3 (Aldrich, 99%) and H_3PO_4 (Prolabo, 95%) in a stoichiometric ratio that underwent precipitation induced by ethanol. The AAM and MOA supports were filled with the CsH_2PO_4 salt by wet impregnation or an ultrasonic bath, where samples were placed in a saturated CsH_2PO_4 aqueous solution for different amounts of time. Then before assembly with the electrodes, the membranes were air dried for differing amounts of time.

2.2. Characterization of supports and composite membranes

The phase compositions of the AAM and MOA supports were analyzed by X-ray diffraction (XRD; model D/max-3C), using a Cu Kα (1.5418 Å) radiation source. The operating voltage and current were 40 kV and 30 mA, respectively. The surface topography and cross-sectional morphologies of the two composite membranes were characterized by a scanning electron microscopy (SEM; Hitachi S-4700) using an electron beam with an energy of 15 keV. Energy dispersion spectrometry (EDS) attached to the SEM was used to detect the elemental distribution.

2.3. Characterization of SAFC performance

The composite membranes of AAM/CsH_2PO_4 and MOA/CsH_2PO_4 were sandwiched between two silver-net current collectors covered with a mixture of Pt black/C black/CsH_2PO_4. The weight ratio of W(Pt):W(C):W(CsH_2PO_4) was 8:9:3, and this mixture was stirred in isopropanol for at least 1 h. The catalyst loading was 1.5 m g cm^{-2} of black platinum. The active area was 1.15 cm^2 and delimited using insulating silicon rubber. The membrane electrode assembly was then placed in a single fuel cell apparatus and fed with oxygen (99.5% purity, 1 bar) and hydrogen (99.5% purity, 1 bar), in a humidified environment at room temperature. Polarization curves were obtained using an M273. Proton conductivities of the composite membranes at room temperature were determined using a Parstat 4000 over a frequency range of 10 Hz to 1 MHz. Data analysis and fitting was performed according to Refs. [9,16] using the ZSimpWin software.

3. Results and discussion

3.1. Morphology and phase characterization of supports

Fig. 1(c)–(f) shows the SEM images and XRD patterns of the AAM and MOA supports. It can be seen from Fig. 1(c) that the nanopores of the AAM support were uniform and highly ordered. In contrast, the morphology of the MOA film, displayed in Fig. 1(d), shows large anomalous pores superposed together, forming a complex and interlaced network structure. It was indicated by the XRD pattern (Fig. 1(e)) that the AAM support consists of amorphous Al_2O_3, as evidenced by a broad peak at 27°. The results in Fig. 1(f) suggest that the MOA support is polycrystalline, given the presence of the α- and γ-Al_2O_3 phases.

3.2. Structural and elemental characteristics of composite membranes

The AAM and MOA supports were filled with the solid CsH_2PO_4 electrolyte and their surfaces and cross-sectional morphologies are shown in Fig. 2 as identified using the SEM. It can be seen from Fig. 2(a) and (c) that the proton conductor CsH_2PO_4 fills the cylindrical pores of the AAM support, forming wire structures. The EDS analysis on the AAM/CsH_2PO_4 cross section confirms the presence of the elements O, Al, P, and Cs, as shown in Fig. 2(e). This result further supports the findings from the SEM images of the AAM/CsH_2PO_4 membrane that suggested CsH_2PO_4 was present inside the pores of the AAM support. Fig. 2(b) shows a large amount of white CsH_2PO_4 crystals covering the surface of the MOA support. The line scan (Fig. 2(f)) of the MOA/CsH_2PO_4 cross section (Fig. 2(d)) revealed that the elements O, Al, P, and Cs were distributed nonuniformly along the membrane cross section. In addition, the MOA/CsH_2PO_4 cross section shown in Fig. 2(d) contains some irregular pores because the solid electrolyte detached in some instances during preparation of the SEM specimens. Based on the characteristics of the MOA support (Fig. 1(d)) and the MOA/CsH_2PO_4 membrane (Fig. 2(b), (d), and (f)), the presence of CsH_2PO_4 inside the MOA support was confirmed. In

Fig. 3 – (a) Polarization curves for AAM/CsH_2PO_4 and MOA/CsH_2PO_4 SAFCs and (b) peak power densities of AAM/CsH_2PO_4 and MOA/CsH_2PO_4 SAFCs as a function of cycle number.

addition, it was determined that an interlaced network inside the MOA support was formed by the proton conductor CsH_2PO_4.

3.3. *Characterization of SAFC performance*

In order to evaluate the performance of a SAFC made from these composite membranes, polarization curves at gas and cell temperatures of 25 °C for a single H_2/O_2 SAFC used with either the AAM/CsH_2PO_4 or MOA/CsH_2PO_4 composite membranes were obtained. As shown in Fig. 3(a), the MOA/CsH_2PO_4 SAFC assembly displayed slightly better results than the AAM/CsH_2PO_4 SAFC assembly, delivering average peak power and conductivity outputs up to 38.5 m W cm^{-2} and 2.1 m S cm^{-1}, respectively, at 25 °C. In light of the literature related to pure solid-acid CsH_2PO_4 fuel cells at room temperature reporting very poor performances ($<10^{-6}$ S cm^{-1}) [9] these results are encouraging. In addition, the interlaced network associated with the CsH_2PO_4 filling inside the MOA support provides better proton transport compared with the wire structure of the CsH_2PO_4 within the AAM support.

Another important aspect that was investigated was the performance stability of the MOA/CsH_2PO_4 fuel cell at 25 °C, which was characterized by recording successive current–voltage (*I*–*V*) characteristics. The peak power densities (P_{max}) of AAM/CsH_2PO_4 and MOA/CsH_2PO_4 SAFCs, as a function of the number of cycles, were compared (Fig. 3(b)). The power values of the AAM/CsH_2PO_4 SAFC sharply decreased down to 10% of their initial values by the 10th curve, owing to the dissolution of both the acidic pore filler and the AAM in the water produced at the cathode–electrolyte interface [7–9]. The solubility of the acidic conductor produced local acidification, which induced the dissolution of the amorphous AAM support. In contrast, the power values of the MOA/CsH_2PO_4 SAFC remained almost constant until the 35th polarization curve was reached. The good stability of the MOA/CsH_2PO_4 SAFC can be attributed to the improved chemical stability of the MOA support, allowing it to avoid acidification arising from the dissolution of CsH_2PO_4. The support's polycrystalline structure was determined using XRD (Fig. 1(d)); it was made up of α- and γ-Al_2O_3 phases that resulted in the MOA having improved chemical stability. The α-Al_2O_3 phase is incapable of dissolving in acid, and its chemical stability is better than that of the amorphous phase Al_2O_3 [17].

In conclusion, although the peak power density and proton conductivity using the MOA/CsH_2PO_4 SAFC assembly were only slightly improved, the strong chemical stability of the MOA support represents progress in the development of composite electrolyte systems for SAFCs.

4. Conclusion

(1) The MOA support was polycrystalline and made up of α- and γ-Al_2O_3 phases; while, the proton conductor CsH_2PO_4 formed an interlaced network within the MOA support.
(2) The average peak power (38.5 m W cm^{-2}) and conductivity (2.1 m S cm^{-1}) of the MOA/CsH_2PO_4 SAFC were slightly better than those of the AAM/CsH_2PO_4 SAFC at room temperature, owing to the interlaced network of CsH_2PO_4 filling the MOA support.
(3) The improved stability of the MOA/CsH_2PO_4 SAFC over the AAM/CsH_2PO_4 SAFC, as measured by recording successive *I*–*V* characteristics, was attributable to the increased chemical resistance of the MOA support afforded by the crystalline α-Al_2O_3 phase.

Acknowledgment

This work was supported by a project of the National Natural Science Foundation (50971126).

REFERENCES

[1] Haile SM, Boysen DA, Chisholm CRI. Solid acids as fuel cell electrolytes. Nature 2001;410:910–3.
[2] Boysen DA, Uda T, Chisholm CRI, Haile SM. High-performance solid acid fuel cells through humidity stabilization. Science 2004;303:68–70.
[3] Uda T, Haile SM. Thin-membrane solid-acid fuel cell. Electrochem Solid-state Lett 2005;8:A245–6.
[4] Uda T, Boysen DA, Chisholm CRI, Haile SM. Alcohol fuel cells at optimal temperatures. Electrochem Solid-state Lett 2006;9:A261–4.
[5] Ahn YS, Mangani IR, Park CW, Kim J. Study on the morphology of CsH_2PO_4 using the mixture of methanol and polyols. J Power Sources 2006;163:107–12.
[6] Yoshimi S, Matsui T, Kikuchi R. Temperature and humidity dependence of the electrode polarization in intermediate-temperature fuel cells employing CsH_2PO_4/SiP_2O_7-based composite electrolytes. J Power Sources 2008;179:497–503.
[7] Bocchetta P, Chiavarotti G, Masi R. Nanoporous alumina membranes filled with solid acid for thin film fuel cells at intermediate temperatures. Electrochem Commun 2004;6:923–8.
[8] Bocchetta P, Ferraro R, Quarto FD. Nanoscale membrane electrode assemblies based on porous anodic alumina for hydrogen–oxygen fuel cell. J Solid State Electrochem 2007;11:1253–61.
[9] Bocchetta P, Ferraro R, Quarto FD. Advances in anodic alumina membranes thin film fuel cell: CsH_2PO_4 pore-filler as proton conductor at room temperature. J Power Sources 2009;187:49–56.
[10] Bocchetta P, Conciauro F, Santamaria M, Quarto FD. $Cs_{0.86}(NH_4)_{1.14}SO_4Te(OH)_6$ in porous anodic alumina for micro fuel cell applications. Electrochim Acta 2011;56:3845–51.
[11] Du KQ, Guo XH, Guo QZ, Wang FH, Tian Y. A monolayer PEO coating on 2024 Al alloy by transient self-feedback control mode. Mater Lett 2013;91:45–9.
[12] Du KQ, Guo XH, Guo QZ, Wang Y, Wang FH, Tian Y. Effect of PEO coating microstructure on corrosion of Al 2024 Corrosion Science and Technology. J Electrochem Soc 2012;159:C597–606.
[13] Guo XH, Du KQ, Guo QZ, Wang Y, Wang FH. Effect of carrier waveform frequency on the microstructure of Al_2O_3 plasma electrolytic oxidation films. ECS Electrochem Lett 2013;2:C11–4.
[14] Guo XH, Du KQ, Ge H, Guo QZ, Wang Y, Wang FH. Good sensitivity and high stability of humidity sensor using micro-arc oxidation alumina film. Electrochem Commun 2013;28:95–9.

[15] Yang PX, An MZ, Zheng TS. Preparation of porous anodic alumina templates using a sulfuric/oxalic acid mixture as electrolyte. Chin J Inorg Chem 2005;21:1907–11.
[16] Springer TE, Zawodzinski TA, Wilson MS, Gottesfeld S. Characterization of polymer electrolyte fuel cells using AC impedance spectroscopy. J Electrochem Soc 1996;145:587–99.
[17] Jin FY, Wang K, Zhu M, Shen LR, Li J, Hong HH, et al. Infrared reflection by alumina films produced on aluminum alloy by plasma electrolytic oxidation. Mater Chem Phys 2009;114:398–401.